BIOLOGY OF REPRODUCTION (2016) **95**(1):16, 1–10
Published online before print 8 June 2016.
DOI 10.1095/biolreprod.115.137109

Quiescence Loosens Epigenetic Constraints in Bovine Somatic Cells and Improves Their Reprogramming into Totipotency[1]

Prasanna K. Kallingappa,[3] Pavla M. Turner,[3] Michael P. Eichenlaub,[4] Andria L. Green, Fleur C. Oback, Alice M. Chibnall, David N. Wells, and Björn Oback[2]

AgResearch Ltd., Ruakura Research Centre, Reproductive Technologies, Hamilton, New Zealand

ABSTRACT

Reprogramming by nuclear transfer (NT) cloning forces cells to lose their lineage-specific epigenetic marks and reacquire totipotency. This process often produces molecular anomalies that compromise clone development. We hypothesized that quiescence alters the epigenetic status of somatic NT donor cells and elevates their reprogrammability. To test this idea, we compared chromatin composition and cloning efficiency of serum-starved quiescent (G_0) fibroblasts versus nonstarved mitotically selected (G_1) controls. We show that G_0 chromatin contains reduced levels of Polycomb group proteins EED, SUZ12, PHC1, and RING2, as well as histone variant H2A.Z. Using quantitative confocal immunofluorescence microscopy and fluorometric enzyme-linked immunosorbent assay, we further show that G_0 induced DNA and histone hypomethylation, specifically at H3K4me3, H3K9me2/3 and H3K27me3, but not H3K9me1. Collectively, these changes resulted in a more relaxed G_0 chromatin state. Following NT, G_0 donors developed into blastocysts that retained H3K9me3 hypomethylation, both in the inner cell mass and trophectoderm. G_0 blastocysts from different cell types and cell lines developed significantly better into adult offspring. In conclusion, serum starvation induced epigenetic changes, specifically hypotrimethylation, that provide a mechanistic correlate for increased somatic cell reprogrammability.

cell cycle, epigenetics, histone modifications, nuclear transfer, reprogramming

INTRODUCTION

During differentiation, somatic genomes acquire highly specialized epigenetic modifications of DNA and DNA-binding proteins [1]. These modifications regulate access to the genetic information, resulting in loss of cell plasticity and stable lineage restrictions. Consequently, differentiated cells rarely switch cell fates or produce daughter cells that do so. Radical manipulations, such as cloning by somatic cell nuclear transfer (SCNT), force cells to lose their lineage-specific epigenetic marks and become totipotent again [2]. During nuclear transfer (NT), a donor nucleus is transplanted into an enucleated oocyte (cytoplast) where its epigenetic marks are cleared by ill-defined reprogramming factors. When this process is incomplete, it leads to aberrant methylation patterns of DNA [3, 4] and histones [5], dysregulation of gene expression [6], and compromised development of the cloned embryo [7]. Development after SCNT can thus serve as a functional bioassay for genomewide epigenetic reprogramming.

The role of specific epigenetic marks as barriers to restoring totipotency remains poorly understood. One aspect that has been particularly controversial is the link between donor cell division and epigenetic reprogramming. The most common somatic donors are diploid fibroblasts in the G_1 or G_0 cell cycle phase. G_1 is the intermediate stage between M- and S-phase in dividing cells. G_1 cells may be obtained by various arrest/release-methods based on imposing reversible metabolic blocks or by mitotic shake-off [8]. By contrast, quiescent (G_0) cells neither grow nor proliferate [9]. This state is commonly initiated by mitogen depletion (e.g., serum starvation) and characterized by specific transcriptional [10, 11] and metabolic [12] changes.

The first adult mammalian SCNT clone, Dolly the sheep, was derived from a serum-starved mammary gland cell [13]. Originally, it had been claimed that using G_0 cells was a major factor contributing to cloning success [13]. This was supported by in vitro mouse NT studies using naturally quiescent donors [14]. However, cloned offspring have also been produced from mitotically selected [15, 16] or proliferating cells [17–19], contradicting earlier claims about the beneficial effect of G_0. Thus, it is unclear which cell cycle stage is more amenable to epigenetic reprogramming.

We hypothesized that serum starvation alters the epigenetic constraints imposed on the genome during differentiation and elevates their reprogrammability. In order to test this idea, we compared chromatin composition of isogenic G_0 versus G_1 donor cells and cloned embryos derived thereof. We focused on 1) Polycomb group (PcG) proteins, 2) posttranslational histone modifications, specifically methylation and acetylation of lysines, and 3) DNA methylation. PcG proteins form multimeric Polycomb repressive complexes (PRCs) that recognize silent target genes and stably lock the surrounding chromatin in a repressed state [20]. The more variable PRC1, made up of core components PHC and RING, maintains transcriptional repression [21]. PRC2, including EED, SUZ12, RBBP4/7, and histone methyltransferase (HMT) EZH1/2, initiates gene silencing through trimethylating (me3) histone (H) 3 at lysine (K) 27 (H3K27me3) [22]. Specific histone methylation sites are either associated with open chromatin and

[1]This work was funded by MSI contracts C10X0303, C10X1002, and AgResearch.
[2]Correspondence: Björn Oback, AgResearch Ltd., Ruakura Research Centre, Reproductive Technologies, Private Bag 3123, Hamilton, New Zealand. E-mail: bjorn.oback@agresearch.co.nz
[3]Current address: The University of Auckland, Faculty of Medical and Health Sciences, Private Bag 92019, Auckland 1142, New Zealand.
[4]Current address: Australian Regenerative Medicine Institute (ARMI), 23 Innovation Walk, Monash University, Wellington Road, Clayton 3800, Australia.

Received: 16 November 2015.
First decision: 20 December 2015.
Accepted: 17 May 2016.

eISSN: 1529-7268 http://www.biolreprod.org
ISSN: 0006-3363

transcriptional activation (e.g., H3K4) or with condensed chromatin and transcriptional repression (e.g., H3K9 and H3K27) [23]. Deacetylation of histone tails correlates with chromatin compaction and suppressed transcription while hyperacetylation loosens the nucleosomal core structure, facilitating RNA polymerase II (Pol II) binding and gene expression [24]. Together with a range of other posttranslational histone marks, these modifications dynamically modulate chromatin structure and function, contributing to changes in gene expression [25, 26].

Here we show that serum starvation globally reduces PcG proteins, histone, and DNA methylation in bovine fibroblasts. Specifically, H3K9me3 hypomethylation persisted in NT-derived embryos and correlated with their increased survival into cloned cattle. These results establish low H3K9me3 as a molecular correlate linking cellular quiescence and improved epigenetic reprogrammability into totipotency.

MATERIALS AND METHODS

Animal Studies

All animal studies were undertaken in compliance with New Zealand laws and were approved by the Ruakura Animal Ethics Committee.

Nuclear Donor Cells

Four adult ear skin fibroblast (LJ801, 3XTC, Age^+, Age^-) and one ovarian follicular (J1) cell line were used as donors for NT (Supplemental Table S1; Supplemental Data are available online at www.biolreprod.org). Cells were isolated and synchronized as described previously [27]. Briefly, G_0 cells were obtained by culture in medium containing 0.5% fetal calf serum (FCS) for 5 days and harvested by trypsinization. Mechanically synchronized G_1 control cells were generated by seeding 10^4 cells/cm^2, culture for 20 h, washing once with PBS, and culturing for another 2 h before mitotic shake-off by gentle tapping. For NT or immunofluorescence (IF), manually selected cell doublets were replated and allowed to complete cytokinesis for 2–3 h before fusion or fixation, respectively. For enzyme-linked immunosorbent assay (ELISA), single mitotic cells and doublets were replated and harvested within 2–3 h after mitotic shake-off.

Cell Proliferation Assays

Cells were seeded at 2.5×10^4 cells/cm^2 and then either left in 10% FCS culture medium or changed to 0.5% FCS medium 17–20 h later. At daily intervals, nonstarved and starved cells were trypsinized and counted in a hemocytometer until they reached the plateau phase. Following mitotic selection, DNA replication was assessed using a 5-Bromo-2-deoxyuridine (BrdU) Cell Proliferation Kit I (Roche Diagnostics) or a click-iT 5-ethynyl-2′-deoxyuridine (EdU) assay (Life Technologies) and counted in at least 10 random fields of view. Cells stained without BrdU/EdU labeling served as a negative control. Real-time changes in cell number, viability, and morphology were quantified using a noninvasive RTCA-SP xCELLigence system (Roche), displaying changes in substrate occupancy as cell index (CI) values. Cells were seeded onto 96-well E-Plates, and CI readings were taken every 1 h. After 6 days in culture, cells were restimulated with 10% FCS. Curves were normalized on the respective CI values 30 min after serum withdrawal.

Quantitative IF

For each comparison, G_0 versus G_1 LJ801 cells were passaged, processed, and analyzed in parallel. G_0 and G_1 cells were plated on coverslips, coated with 1:2 ratio of 2.5% collagen and 0.1% gelatin, and allowed to settle for 2–3 h. Cells and embryos were treated with 3.6% (w/v) paraformaldehyde/1% (w/w) Triton X-100 in PBS for 10 min, blocked with 2.5% (w/v) bovine serum albumin in PBS, and incubated overnight at 4°C–8°C with primary antibodies (Supplemental Table S2). The next day, cells were washed in PBS and incubated for 1 h at room temperature with Alexa Fluor 488 or 568 donkey anti-goat, -mouse, -rabbit, or -sheep secondary immunoglobulin G antibodies (Life Technologies). DNA was counterstained with 5 μg/ml Hoechst 33342 (Sigma). Preparations were washed in PBS and water before mounting (DAKO, Med-Bio Ltd.). For 5-methylcytosine (5mC), IF was performed as described [28] and nuclei counterstained with a mix of 1 μg/ml 4′,6-diamidino-2-phenylindole (Sigma) and Hoechst 33342. Negative controls were processed the same way except that the primary antibodies were replaced with blocking buffer. Wide-field epifluorescence (Olympus BX50), images were captured with a digital camera (Spot RT-KE slider) and processed using Spot software (v4.6). For quantitation, confocal images were acquired with all microscope and laser settings kept constant between technical replicates. Pixel intensity of single confocal frames from randomly selected nuclei was quantified (Olympus FluoView FV1000 with FV10-ASW 1.4 software) and normalized on DNA signal (Hoechst 33342) or area (for 5mC staining). First, one random cytoplasmic area was background-subtracted from each image. The nucleus was marked as the region of interest, and series analysis was performed to compute the area and average intensity of the entire stack. Within each stack, the frame of highest average pixel intensity for the antibody channel was selected and divided by the corresponding Hoechst 33342 pixel intensity. As a control, all pixel intensity data were also normalized on nuclear area. This changed the absolute values but not the significance of the results (data not shown). For inner cell mass (ICM) and trophectoderm (TE) quantification of LJ801-derived NT and in vitro fertilized (IVF) blastocysts, nuclei on the inside and outside of the blastocyst, respectively, were randomly selected from the DNA channel. DNA was counterstained with Hoechst 33342. Each image represents a single representative frame from a complete confocal z-series. To assess chromatin condensation, random line selection was used to pass through the region of interest in the H33342 channel. Intensity profiles were plotted as the moving average of 100 pixels.

ELISA

Histones were extracted using an EpiQuik total histone extraction kit. The amount of histone methylation was quantified with EpiQuik Global Histone Methylation Assay Kits (Epigentek) for H3K4me3, H3K9me1, H3K9me2, H3K9me3, and H3K27me3 on a BioTek Synergy 2 Microplate Reader by comparing to a kit standard according to the manufacturer's guidelines.

Generation of NT Embryos and Calves

For IF analysis and embryo transfer (ET), zona-free NT [29] and zona-intact NT [27], respectively, were performed as described. Briefly, in vitro matured (IVM) nonactivated metaphase II (MII)-arrested oocytes were derived from ovaries of slaughtered mature cows [29]. After IVM for 18–20 h, the cumulus-corona was dispersed by vortexing in bovine testicular hyaluronidase. Oocytes with a first polar body were chosen for enucleation. At 23–25 h after the start of IVM, couplets were automatically aligned and electrically fused at 2.0 kV/cm. Reconstructed SCNT embryos were artificially activated 3–4 h postfusion, using a combination of ionomycin and 6-dimethylaminopurine. After 4 h in 6-dimethylaminopurine, reconstructs were washed three times in hepes-buffered synthetic oviduct fluid (HSOF) and transferred into AgResearch-SOF culture medium droplets [27], either singularly (for zona-free NT) or in groups of 10 (for zona-intact NT), for sequential in vitro culture. Embryo cultures were overlaid with mineral oil and kept in a humidified modular incubation chamber (ICN Biomedicals Inc.) gassed with 5% CO_2, 7% O_2, and 88% N_2. In vitro development was assessed on Day 7 (D7) after fusion, and morphological grade 1–2 quality embryos were nonsurgically transferred singularly to synchronized recipient cows [29]. Fetal development was monitored by regular ultrasonography and rectal palpation throughout gestation.

In Vitro Fertilization

IVM oocytes from slaughterhouse ovaries of mixed breed dairy cows were fertilized with frozen-thawed semen from a sire with proven in vitro fertility as described [30]. For sequential in vitro culture, 10 IVF embryos were pooled in 20 μl of AgResearch-SOF as described [31], Embryos were morphologically graded on D7 [32], and morphological grade 1–2 quality embryos were used for gene expression analysis or quantitative IF.

Quantitative RT-PCR

Single grade 1–2 blastocysts were lysed in TRIzol (Thermo Fisher Scientific) and cDNA synthesized as described [33]. Reverse transcriptase was omitted in one sample each time a batch was processed for cDNA synthesis. Primers were designed using NCBI/ Primer-BLAST (Supplemental Table S3) and synthesized by Integrated DNA Technologies. For quantitative RT-PCR, a LightCycler 2.0 (Roche) was used. All reactions were performed with the LightCycler FastStart DNA MasterPLUS SYBR Green I Kit. The ready-to-use Hot Start reaction mix consisted of 0.4 μl of each primer (10 μM), 2.0 μl master mix, 6.2 μl diethylpyrocarbonate-treated water, and 1.0 μl cDNA template. The

following four-segment program was used: 1) denaturation (10 min at 95°C); 2) amplification and quantification (20 sec at 95°C, 20 sec at 60°C, followed by 20 sec at 72°C with a single fluorescent measurement, repeated 45 times); 3) melting curve (95°C, then cooling to 65°C for 20 sec, heating at 0.2°C sec^{-1} to 95°C while continuously measuring fluorescence); and 4) cooling to 4°C. Product identity was confirmed by gel electrophoresis and melting curve analysis. For relative quantification, external standard curves were generated from five serial 10-fold dilutions for each gene in duplicate. One high-efficiency curve ($3.6 \geq$ slope ≥ 3.1, $R^2 > 0.99$) was saved for each target gene and imported for relative quantification compared to 18S RNA as described [33].

Statistical Analysis

Antigen data were analyzed using one-way ANOVA with equal variance. Error bars represent either mean ± SEM or least significant difference (LSD) at 5%. If the LSD bar does not intersect two data midpoints, then the difference between them is $P < 0.05$. For comparing NT versus IVF embryos by quantitative IF, standard errors of the ratios (SER) were calculated as SER (x/y) = (x/y)*$\sqrt{(CV(x) \wedge 2 + CV(y) \wedge 2.)}$ with CV = coefficient of variation = SEM/mean. The quantitative RT-PCR data were analyzed by two-tailed *t*-tests. Development data were analyzed using the two-tailed Fisher exact test for independence in 2 × 2 tables. Significance was accepted as $P < 0.05$. Unless stated otherwise, ''N'' denotes the number of samples analyzed; ''n'' denotes the number of replicate experiments.

RESULTS

G_0 Versus G_1 Donors

We first characterized the cell cycle status of serum-starved donors. Six days after subculture, nonstarved fibroblasts and follicular cells plateaued at saturation density, while starved cells significantly reduced proliferation at much lower density, indicating that this was not due to physical crowding in the dish (Supplemental Fig. S1A). Serum starvation significantly reduced the proportion of cells incorporating BrdU in S-phase compared to culture medium with 10% FCS (Supplemental Fig. S1, B and C). Reversibility of the quiescent state was characterized for fibroblasts using noninvasive real-time kinetic cell profiling. Serum-deprivation prevented cell proliferation compared to control cells. Following addition of 10% FCS after 5 days of starvation, cells reentered a typical growth curve, similar to nonstarved populations (Supplemental Fig. S1D). The proportion of S-phase fibroblasts did not increase even when the cells were starved for up to 10 days in the continuous presence of BrdU label (Supplemental Fig. S1E). Next, manually selected mitotic control cells were characterized to ascertain that they were in G_1 phase. None of the fully cleaved fibroblasts had incorporated BrdU within 3 h of continuous labeling after mitotic selection (Supplemental Fig. S2A). The selected population had not entered quiescence or died as BrdU labeling for 12 h postmitosis demonstrated almost complete progression into S-phase. Cell numbers increased from 3 to 12 h and 24 h postmitosis, indicating normal progression of the cell division cycle (Supplemental Fig. S2B). For large-scale biochemical studies all mitotic cells dislodged by mitotic shake-off were collected because it was impractical to manually select cell doublets. This resulted in a slightly increased contamination with S-phase cells compared to manual selection, while the proportion of cells that progressed into the S-phase after 24 h remained similar (Supplemental Fig. S2C). Thus, mitotically selected control donors were largely captured in G_1, that is, postmitosis and prior to S-phase.

Following this initial characterization, we compared global chromatin status in G_0 versus G_1 control cells. By measuring total Hoechst 33342 pixel intensity, we found that G_0 nuclei contained the same amount of DNA as G_1 nuclei (Supplemental Fig. S3A). However, G_0 DNA was spread over a larger volume than in G_1 nuclei, suggesting a more relaxed chromatin configuration in G_0 (Supplemental Fig. S3B). Using increased Hoechst 33342 pixel intensity as a proxy for increased chromatin condensation, G_1 nuclei showed a shifted peak and overall pixel distribution toward more intense signals (Supplemental Fig. S3C), indicating their more compact chromatin state.

Chromatin Proteins in G_0

Transcriptionally repressive PcG proteins, in particular PRC1-complex component RING2, have been directly implicated in higher-order chromatin compaction [34]. We therefore quantified the abundance of several candidate PcG proteins in G_0 versus G_1 cells. Using confocal IF, we found that PRC2 (EED, EZH2, SUZ12) and PRC1 (PHC1, RING2) protein levels were on average halved in G_0 nuclei, consistent with their less compact chromatin state (Fig. 1A). For each chromatin protein, an average 20 G_0 versus 18 G_1 nuclei were quantified (n = 3–7 replicates), and with the exception of EZH2 ($P = 0.12$), the reduction in PcG levels G_0 nuclei was significant (Fig. 1B). Another chromatin protein linked to promoting chromatin compaction is the histone variant H2A.Z [35]. Similar to RING2, H2A.Z abundance was also about halved in G_0 nuclei (Supplemental Fig. S4A). RNA Pol II, a chromatin-remodeling enzyme that catalyzes the synthesis of mRNA, was significantly less abundant in G_0 cells (Supplemental Fig. S4B).

Chromatin Modifications in G_0

The mammalian PRC2 complex catalyzes mono-, di-, and trimethylation of H3K27 in mammalian cells through the activity of the histone methyltransferases EZH2 and EZH1 [36]. Therefore, we investigated the abundance of active and repressive posttranslational histone methylations in G_0 versus G_1 cells using confocal IF (Fig. 2A). Comparing G_0 versus G_1 nuclei (N = 30 vs. 20 for G_0 vs. G_1, respectively, n = 3–7), the amount of global H3/4K-methylation, H3K4me3, H3K9me2/3, and H3K27me3 was about halved in G_0 chromatin, similar to the reduction in PcG proteins. Only H3K9me1 levels were slightly, but not significantly, elevated (Fig. 2B). To validate these results by an independent biochemical method, we measured the relative abundance of modified histones by fluorometric ELISA using nuclear extracts of G_0 and G_1 cells (Fig. 2C). With the exception of H3K9me1, all other histone methylation levels (H3K4me3, H3K9me2/3, and H3K27me3) were significantly reduced in G_0 versus G_1, confirming our previous IF results. Comparing both methods, the relative G_1/G_0 ratios consistently showed the same trend for both IF and ELISA, while absolute ratios were on average ~25% less with ELISA (Fig. 2D).

In contrast to the uniform reduction in trimethylation levels, alterations in histone acetylation were less consistent (Supplemental Fig. S5A). While H3K9ac was 2.7-fold reduced in G_0 versus G_1 (N = 21 vs. 28 nuclei quantified, respectively), H4 acetylation was either reduced (H4K5ac, 4.2-fold, N = 10 vs. 12), unchanged (H4K16ac, N = 20 vs. 31) or increased (H4K12ac, 2.2-fold, N = 11 vs. 16) (Supplemental Fig. S5B). In mammals, HDAC1 deacetylates H4K5 and initiates transcriptional repression [37]. Despite the reduction in H4K5ac, we did not observe an increase in HDAC1 levels (N = 8 G_0 vs. 12 G_1 nuclei) (Supplemental Fig. S5B).

Histone- and DNA-methylation are mechanistically linked. For example, DNA methylation requires the interaction of hemi-methylated DNA, DNA methyltransferase 1 (DNMT1), and H3K9me2/3 [38], especially at pericentric heterochromatin

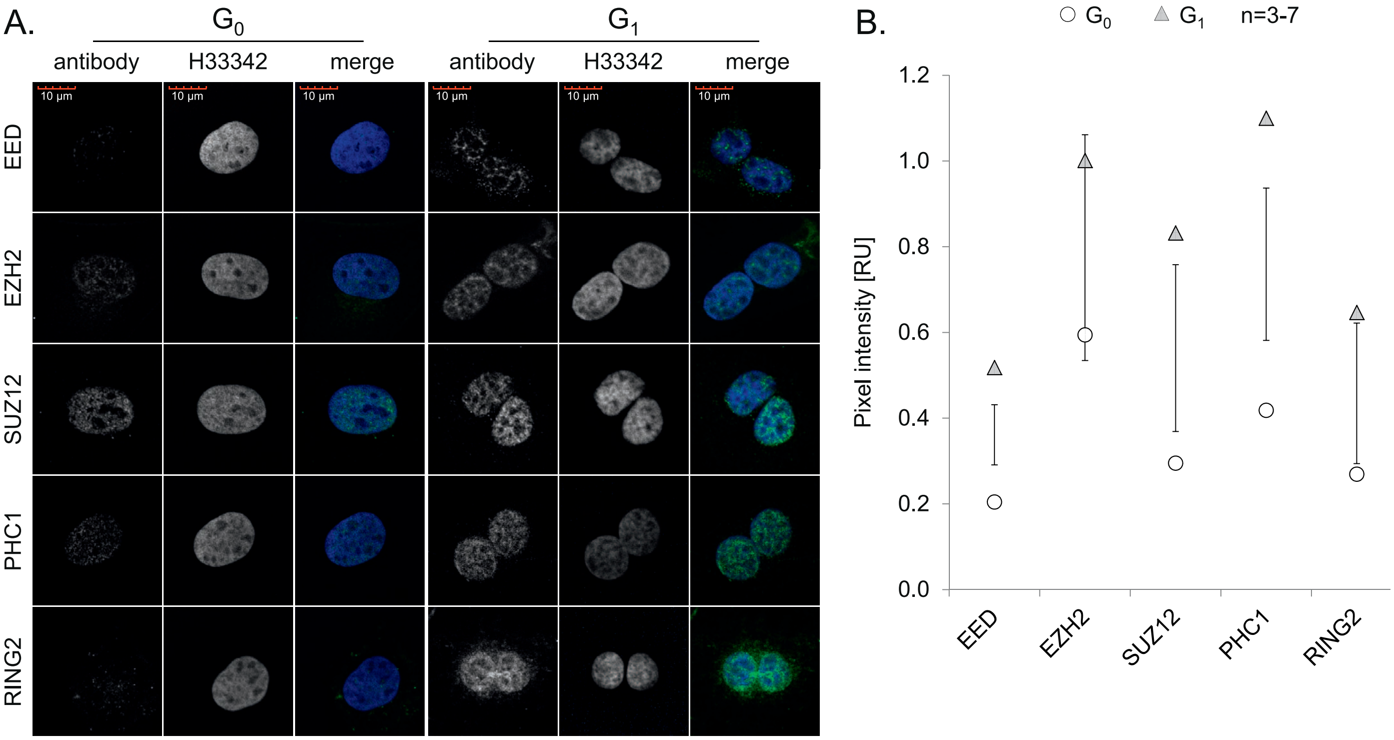

FIG. 1. PcG protein levels are globally reduced in G_0. **A**) Confocal IF images of PRC2 (EED, EZH2, SUZ12) and PRC1 (PHC1, RING2) components (antibody) in G_0 versus G_1 cells. DNA was counterstained with Hoechst 33342 (H33342) and the merged image shown in color, with blue: DNA and green: antibody (merge). Each image shows a single representative frame from a complete confocal z-series. **B**) Quantitative confocal IF. Mean G_0 versus G_1 values are separated by least significant difference (LSD) bars. If the LSD bar does not intersect two data midpoints, then the difference between them is $P < 0.05$. Most PcG proteins were significantly reduced ($P < 0.05$) in G_0 versus G_1 (EED: 20 vs. 19; EZH2: 26 vs. 19; SUZ12: 22 vs. 19; PHC1: 24 vs. 18; RING2: 18 vs. 14 nuclei quantified, respectively), circles = G_0, triangles = G_1; RU = relative units; n = no. replicates.

[39]. In turn, DNA methylation is necessary for stable perpetuation of noncentromeric H3K9me3 [40]. We found that 5mC and H3K9me3 closely colocalized at intranuclear foci in G_0 versus G_1 cells (Supplemental Fig. S5C). Concomitantly with the loss of H3K9me3 in G_0, 5mC was also about 2-fold reduced in quiescent cells (N = 18 vs. 28 for G_0 vs. G_1, respectively) (Supplemental Fig. S5B).

Chromatin Reprogramming in G_0 Embryos

We next sought to determine how this more relaxed epigenetic fingerprint in G_0 donors was reprogrammed during NT cloning. Minutes after transfer into recipient oocytes, Hoechst-stained G_0 DNA was still in its interphase configuration, while G_1 DNA had already assumed the metaphaselike state characteristic of premature chromatin condensation (PCC) (Supplemental Fig. S6A). This delayed chromosome condensation in G_0 donors was likely due to their more relaxed initial chromatin configuration. At this early stage after NT, trimethylated H3K4, H3K9, and H3K27 remained reduced in G_0-derived embryos (Supplemental Fig. S6A), indicating that neither remethylation of G_0 nor demethylation of G_1 histones were immediately obvious events. We analyzed reprogramming of chromatin proteins and modifications again when NT reconstructs had developed into blastocysts with an outer epithelial TE layer and ICM. Using confocal IF, we compared G_0- versus G_1-derived blastocysts (Fig. 3A). Irrespective of the original donor cell stage, all NT blastocysts showed globally hypomethylated ICM compared to TE nuclei (Fig. 3B). Importantly, only H3K9me3 remained hypomethylated in G_0- versus G_1-derived whole NT blastocysts, both in the ICM and TE ($P \leq 0.05$). H3K4me3 and H3K27me3, on the other hand, were equally reprogrammed in blastocysts. With respect to PcG proteins, SUZ12 remained down-regulated in the ICM of G_0-derived blastocysts ($P < 0.005$), while the initial donor differences for RING2 were no longer detectable. For these quantifications, an average 48 and 98 G_0 versus 36 and 72 G_1 ICM and TE nuclei, respectively, were analyzed in two to seven replicates.

As a benchmark control for developmentally more competent embryos, we analyzed IVF blastocysts by quantitative confocal IF for H3K4me3, H3K9me3, H3K27me3, RING2, and SUZ12 (Supplemental Fig. S7A). SUZ12 and H3K27me3 levels were consistently lower in NT embryos, especially in G_0 ICMs and G_0 whole blastocysts (Supplemental Fig. S7B). For H3K9me3, G_0 versus G_1 embryos were hypo- versus hypermethylated, respectively, but this change was not significant compared to IVF controls (Supplemental Fig. S7B).

Epigenetic changes often affect transcription. We analyzed candidate gene expression in G_0/G_1-derived blastocysts (Supplemental Fig. S8), including pluripotency markers (*NANOG*, *SOX2*, *DPPA3*, *IFITM3*) [41–44], as well as an imprinted gene (*SNRPN*) with reduced DNA methylation in SCNT fetuses [45] and an H3K9me3 demethylase (*KDM4B*) that promotes reprogramming [46]. None of these differed significantly between G_0- versus G_1-derived blastocysts (22 G_0 vs. 38 G_1 blastocysts, n = 4). Transcripts for other H3K9me3 demethylases (*KDM4A*, *KDM4C*, and *KDM4D*) were not reliably detected in blastocysts, using two different primer pairs for each target (data not shown).

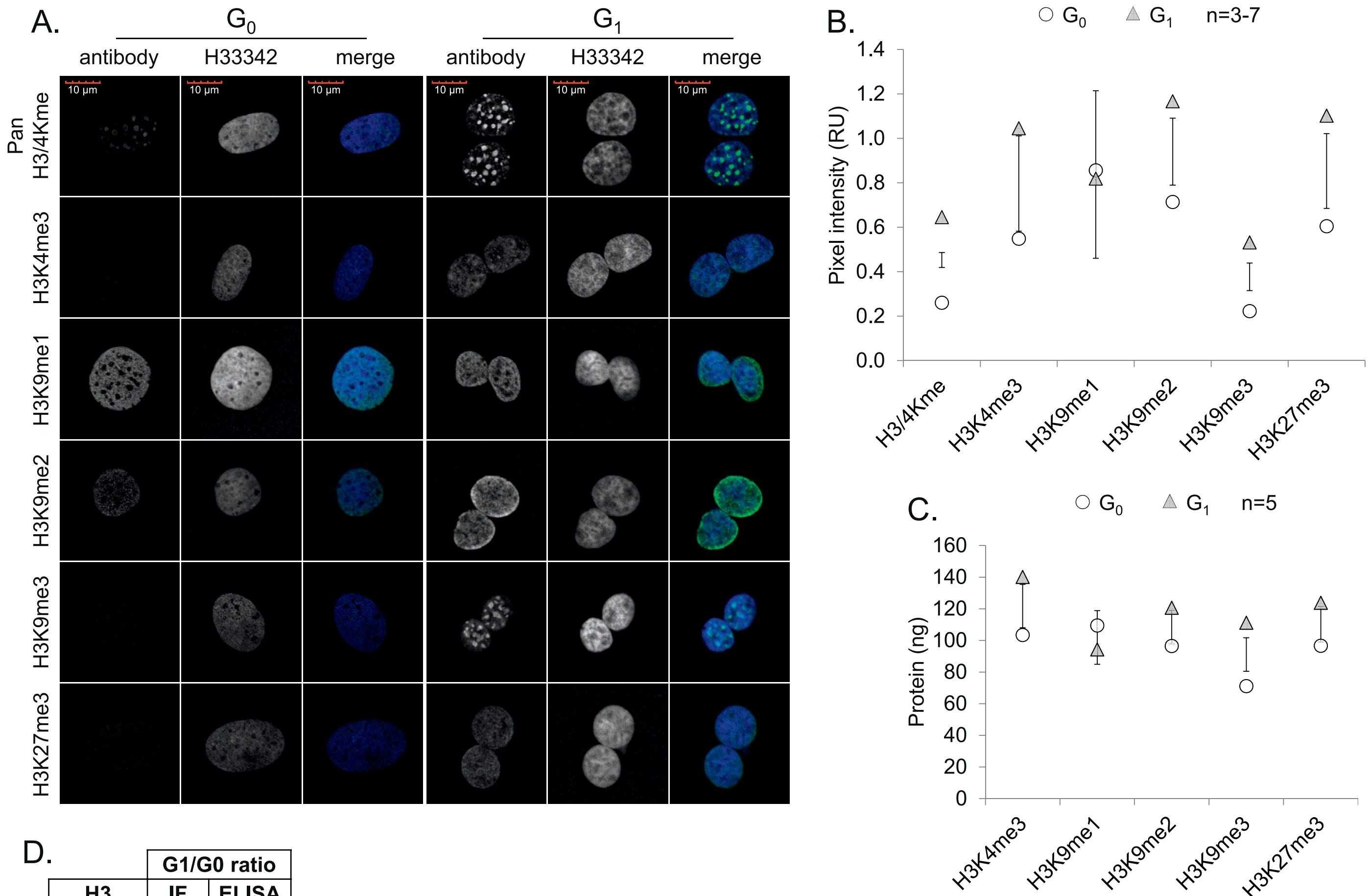

D.

	G1/G0 ratio	
H3	IF	ELISA
K4me3	1.91	1.35
K9me1	0.96	0.86
K9me2	1.64	1.25
K9me3	2.39	1.56
K27me3	1.82	1.28

FIG. 2. Histone methylation levels are globally reduced in G_0. **A**) Confocal IF images of methylated pan-H3/4K, H3K4, H3K9, and H3K27 epitopes (antibody) in G_0 versus G_1 cells. DNA was counterstained with H33342 and the merged image shown in color, with blue: DNA and green: antibody (merge). Each image shows a single representative frame from a complete confocal z-series. **B**) Quantitative confocal IF. Mean G_0 versus G_1 values are separated by LSD bars. Most histone methylation levels were significantly reduced ($P < 0.05$) in G_0 versus G_1 (H3/4Kme: 21 vs. 15; H3K4me3: 40 vs. 26; H3K9me1: 38 vs. 29; H3K9me2 18 vs. 13; H3K9me3: 46 vs. 22; H3K27me3: 28 vs. 16 nuclei quantified, respectively), circles = G_0, triangles = G_1; RU = relative units. **C**) Relative abundance of modified histones estimated by ELISA with appropriate antibodies using nuclear extracts of G_0 and G_1 cells. Mean G_0 versus G_1 values are separated by LSD bars, circles = G_0, triangles = G_1. Most histone methylation levels are significantly reduced ($P < 0.05$) in G_0 versus G_1; n = no. replicates. **D**) Comparison of G_0/G_1 ratios between IF and ELISA.

G_0 Reprogramming into Totipotency

Progression to certain developmental milestones can serve as a functional readout to measure the extent of epigenetic reprogramming after NT. For LJ801 fibroblasts, G_0 donors developed slightly better into blastocysts than G_1 donors (198/429 = 46% vs. 154/396 = 39%, respectively, $P < 0.05$, n = 9). However, this was not observed for transferable quality blastocysts (137/429 = 32% vs. 108/396 = 27%, respectively, $P = 0.17$, n = 9) and also not apparent with other cell types and lines (Supplemental Table S4), emphasizing that in vitro blastocyst formation is a poor indicator for developmental competence. Instead, long-term development into live animals is the most meaningful measure of extensive donor cell reprogrammability [47]. For male LJ801 fibroblasts, serum starvation increased survival throughout gestation and in particular postnatal survival into adulthood (Fig. 4A). This trend was also observed for female 3XTC fibroblasts (Supplemental Fig. S9). Across five different cell lines and genotypes (Fig. 4B), G_0 embryos (N = 104) survived significantly better to pregnancy (35 days), term, weaning (3 mo), and adulthood (3 yr) than G_1 embryos (N = 178) (52% vs. 35% [N = 54 vs. 63 pregnant] with $P < 0.01$, 19% vs. 10% [N = 20 vs. 18 born], 14% vs. 6% [N = 15 vs. 10 weaned], and 10% vs. 4% [N = 11 vs. 7 adult animals] with $P < 0.05$, respectively). This trend was also observed for each fibroblast cell line plotted individually and for follicular cells (Supplemental Fig. S9). We did not observe a difference in the occurrence of hydroallantois, the most common complication in bovine SCNT pregnancies in our hands. Likewise, there was no difference in birth weights between the G_0 versus G_1 groups (35.7 vs. 35.8 kg, respectively).

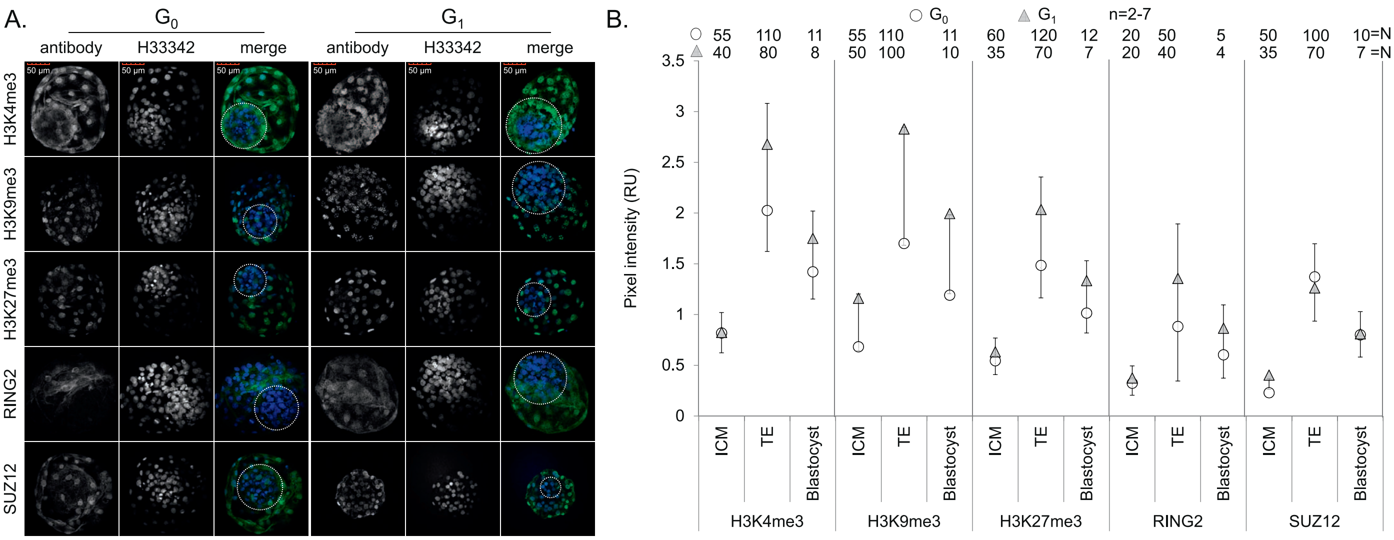

FIG. 3. H3K9me3 levels remain globally reduced in G_0-derived blastocysts. **A**) Confocal IF images of trimethylated H3K4, H3K9, and H3K27 as well as SUZ12 and RING2 (antibody) in G_0- and G_1-derived zona-free blastocysts. DNA was counterstained with H33342 and the merged image shown in color, with blue: DNA and green: antibody (merge). Stippled circle outlines ICM. Each image shows a single representative frame from a complete confocal z-series. **B**) Quantitative confocal IF of optically separated (ICM, TE) and whole (blastocyst) blastocysts. Mean G_0 versus G_1 values are separated by LSD bars. H3K9me3 and SUZ12 are differentially reprogrammed in G_0-derived versus G_1-derived blastocysts; circles = G_0, triangles = G_1; RU = relative units; N = no nuclei analyzed; n = no. replicates.

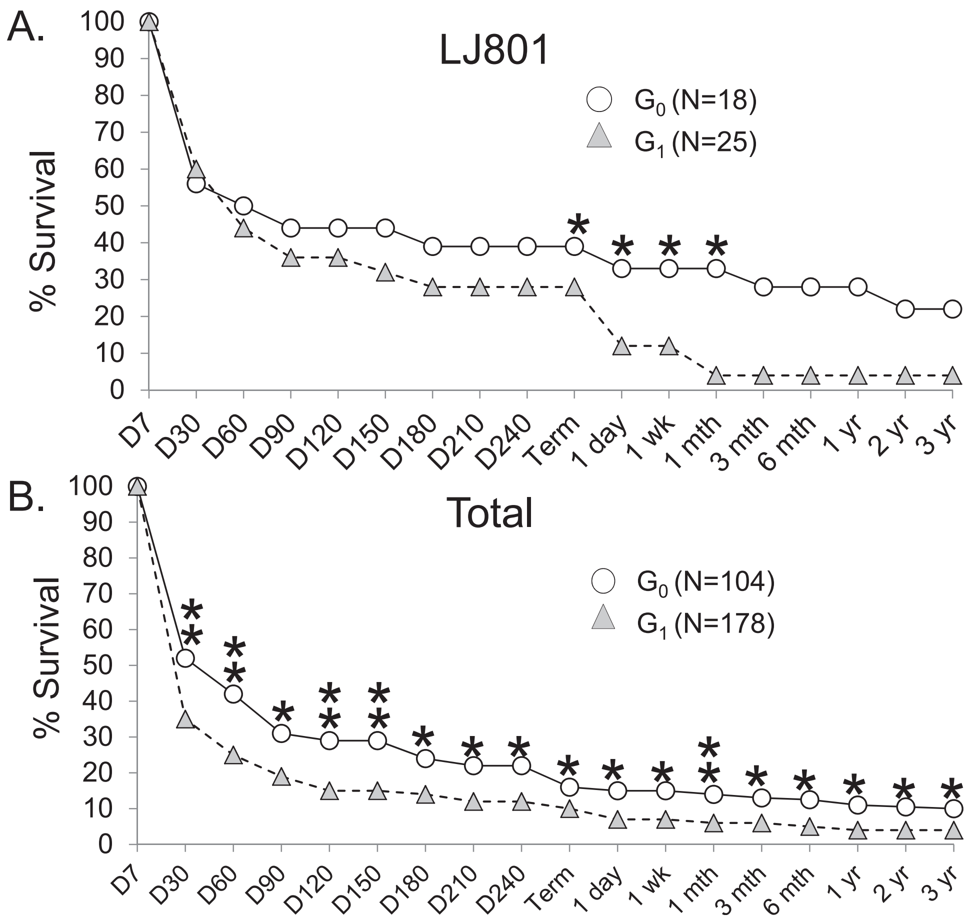

FIG. 4. Survival of bovine clones from D7 into adulthood (3 yr old). Calves were cloned from either G_0 or manually selected G_1 donors. Survival data for individual (LJ801; **A**) or all cell lines (Total = LJ801, 3XTC, Age$^+$, Age$^-$, J1; **B**) are shown. Day of embryo transfer (D7) is set to 100%, N = number of zona-intact embryos transferred; circles = G_0, triangles = G_1; *$P < 0.05$, **$P < 0.01$.

DISCUSSION

Here we show that somatic G_0 cells globally down-regulate chromatin-compacting proteins and histone methylation, resulting in a more relaxed chromatin structure and increased cattle cloning efficiency. This provides a long-sought molecular correlate for the elevated reprogrammability of quiescent donor cells into totipotency.

Cell cycle coordination between the nuclear donor and MII-arrested cytoplast can increase cloning efficiency by 1) maintaining normal chromosome ploidy in the reconstructed NT embryo and 2) promoting epigenetic reprogramming of the donor genome [2]. In order to exclude ploidy-related reprogramming artifacts from G_2/M [16] or S-phase nuclei [16, 48], it was therefore important to ascertain that donors were synchronized in G_0/G_1.

Serum starvation inhibited proliferation in all cell lines, with only a small proportion of fibroblasts (<3%) still synthesizing DNA. Such small refractory subpopulations were observed before [49, 50]. The majority of cells entered a prereplicative quiescent state that was fully reversible upon serum stimulation. It has been suggested that the total cell cycle time lengthens under serum deprivation and that most cells become BrdU positive during an extended labeling interval [51]. However, we found <4% of cells in S-phase, mostly distributed in small scattered clusters of BrdU-labeled cells, even upon starvation for 10 days. This indicates that most cells were quiescent, rather than just cycling slowly. Based on BrdU-labeling alone, the cell cycle stage of those cells that remained unlabeled under serum starvation cannot be deduced. Using dual-parameter fluorescence-activated cell sorting analysis, the majority of serum-starved bovine [50, 52] or porcine fibroblasts [49] contained cells with a G_1 amount of DNA, with the remainder being in G_2/M- and S-phase. By selecting the smallest cells in the serum-starved population, which is our NT practice, the proportion of G_0/G_1 cells further increased [49]. To obtain healthy populations of manually synchronized G_1 cells, we used positive mitotic selection [8]. Throughput with this individual selection method is much lower than with nonselection methods, such as drug-induced G_1-arrest, but it results in a more uniform and defined starting population. Most cells are captured when the chromosomes have already segregated [27], minimizing chromosomal distribution errors (i.e., gain or loss of chromosomes) from manual handling. It is unlikely that any cells had progressed into early S-phase because even short BrdU/EdU incorporation periods (1 min) are clearly detectable [53]. For ELISA, it was necessary to perform high-throughput mitotic shake-off, slightly increasing contamination with S-phase cells compared to manual selection. S-phase cells contain fewer fully methylated histones [54, 55], reducing histone methylation in nuclear G_1 cell extracts. This may explain the decreased absolute G_1/G_0 ratios in the ELISA data. Nevertheless, S-phase contamination, which would have been incompatible with blastocyst development [16], was not enough to significantly compromise in vitro development of G_1 donors. Taken together, both starved and nonstarved donor populations were predominantly captured postmitosis and prior to S-phase with a diploid amount of DNA, minimizing ploidy-related variation.

Serum-starved fibroblasts remain transcriptionally [10, 11] and metabolically [12] highly active. However, little is known about the epigenetic mechanisms governing quiescence. G_0 DNA was spread over a larger nuclear volume than equal amounts of G_1 DNA. This nuclear size difference may have gone unnoticed before because methods to chemically synchronize cells in G_1 do not stop the nucleus from growing [56]. Some reports have identified differences in DNA-binding proteins, such as histone variants [57], HMTs, and PcG proteins that preferentially bind target promoters in G_0 rather than in G_1 cells [58], but these data seem to depend on the method of G_0 arrest [59]. We found that most chromatin-compacting proteins and histone modifications, both activating and repressive, were down-regulated. In line with a more relaxed chromatin configuration in G_0 nuclei, PRC2 components, which catalyze H3K27 methylation in euchromatic regions, as well as PRC1, which is recruited to H3K27me3 regions [60], were down-regulated by half. Reducing the levels of RING2 may be particularly effective at promoting chromatin decondensation and gene derepression [61]. Loss of H2A.Z, which co-occupies RING2 target promoters and favors higher-order chromatin condensation, could further aid in this process [62]. Chromatin dynamics in NT reconstructs further support the notion that it takes longer to condense G_0 than G_1 chromatin. When a G_0/G_1 donor nucleus is introduced into an MII cytoplast, cyclin B/cdk 1 complexes induce PCC. Accordingly, we observed that minutes after NT, G_0 DNA was still in its interphase configuration, while G_1 DNA had already assumed the metaphaselike state characteristic of PCC. This delayed PCC in G_0 donors may be due to their more relaxed initial chromatin configuration.

To facilitate nuclear reprogramming, epigenetic modifications in donor cells have been modified by treating them with various pharmacological histone deacetylase inhibitors, eliciting different responses in mouse SCNT [63]. Some of these agents induce hyperacetylated, transcriptionally permissive chromatin and increase chromosome decondensation and nuclear volume in SCNT embryos [64]. They can also improve cloning efficiency to term in mouse [63] and pig [65]. While histone acetylation was only partially reduced (H3K9ac, H4K5ac) in G_0, the correlation with DNA and histone hypomethylation levels was more consistent. Low DNA and histone methylation is correlated with the naïve pluripotent state in mouse embryonic stem cells [66–68] and also improves cell reprogramming into pluripotency [69–71] and totipotency [46, 72, 73]. The naïve mouse epiblast has a unique epigenetic signature, made up of high DNA hydroxylase levels [74], low expression of DNA methyltransferases [68], and concomitant genome-wide DNA hypomethylation [75]. A similar effect was observed in resting mouse lymphocytes that reduced heterochromatin-associated proteins, PcG components, and H3K4, H3K9, H3K27 as well as H4K20 methylation, culminating in improved development into cloned embryos [14]. In a different context, overexpressing histone lysine demethylases (KDMs) 2A/B, which reduce transcriptionally activating H3K36 and H3K4 methylation marks, increased efficiency of induced pluripotent stem cells reprogramming [76, 77]. Particularly H3K9 marks, which persist through multiple cell divisions [40] pose a critical epigenetic barrier in cell reprogramming. We previously identified H3K9me3-specific KDM4B as a potent enhancer of NT-mediated reprogramming [46]. *Kdm4b*-overexpressing donor cells reduced heterochromatic H3K9me3 levels and reprogrammed better into cloned mouse blastocysts [46]. Similarly, overexpressing *Kdm4d* and depleting H3K9 methyl transferases (KMTs) in mouse SCNT embryos markedly increased SCNT efficiency to term [73]. Reprogramming into induced pluripotent stem cells is also promoted by small interfering RNA-mediated H3K9 KMT knockdown [69, 70, 78], perhaps by restricting initial binding and expression of pluripotency factors located in heterochromatic regions [70]. Targeting KMT1c/G9a and JHDM2A/KDM3A, which both modify H3K9, also showed a beneficial effect on cell reprogramming [79, 80]. Whereas cloned mouse embryos

from *Kdm4b*-overexpressing donors rapidly restored H3K9me3 levels [46], G_0-induced H3K9me3 hypomethylation in cattle persisted as an epigenetic signature until at least the blastocyst stage. This emphasizes species-specific differences in epigenetic reprogramming during normal development, perhaps due to different levels of KMT abundance or activity between oocytes from mouse and cattle. It would be informative to analyze placental, fetal, or newborn/adult tissues for long-term persistence of these epigenetic changes.

Strikingly, global DNA and most histone methylation was about halved in G_0 chromatin (range of G_1/G_0 IF ratio: 1.6–2.4). This could be explained by a cell cycle-related mechanism, whereby cells that acquire nonmethylated histones and hemi-methylated DNA during S-phase would not reinstate these modifications upon serum starvation, despite one parental strand providing a template to do so [54, 55]. It would allow cells to prepare their epigenome for quiescence during a phase of intense chromatin remodeling, enabling them to complete their last DNA replication and mitosis before entering a nonproliferative G_0 state with an already genomewide reduced methylation profile. Outside S-phase, it may be more difficult to synchronize down-regulation of such a large number of epigenetic changes that are associated with quiescence. Such a mechanism may not apply to H3K9me1, which is acquired immediately after nucleosome incorporation and primes subsequent di-and tri-methylation and acetylation, which is much more dynamic [81]. It will be instructive to explore when exactly G_0 cells lose and regain their epigenetic specifications and identify which extrinsic signals trigger these events.

There are additional differences between G_0 versus G_1 cells. For example, serum-starved cells are about 2-fold larger, containing twice the cytoplasmic contents (e.g., mRNA, protein, mitochondria), which could affect reprogramming after NT. However, this volume difference is small relative to the almost ~1000-fold dilution in the much larger cytoplast [82], reducing effects from differential cytoplasmic carryover between G_0 versus G_1 cells. Development into healthy adult offspring measures complete reprogramming of epigenetic modifications required for totipotency. This is the most time-consuming and definitive measure of extensive donor cell reprogramming [47]. It takes into account that cloned animals often show higher postnatal mortality than controls [83, 84], uncovering frailties later in their life. Serum starvation improved epigenetic reprogrammability into live animals. This supports previous findings, which were confounded by 1) comparing G_0 to drug-arrested early and late G_1 cells and 2) different activation timing [27]. By contrast, one study found mitotically arrested G_1 cells superior to confluent cells, based on a relatively small number of embryo transfers [17]. However, 34% of confluent cultures still incorporated BrdU and may thus not have been quiescent [17]. A second study compared serum-starved with roscovitine-treated granulosa cells and also found no significant differences in live births [85]. However, fluorescence-activated cell sorting analysis showed no difference in the G_1- and S-phase fraction between serum-starved and cycling cells, indicating that cells had not entered quiescence. On theoretical grounds, nonselective treatments (e.g., roscovitine) where all cells in a randomly cycling population are treated identically may not actually synchronize cells [86].

In conclusion, serum starvation induced features of a derestricted epigenome that correlated with long-term increased donor cell plasticity and cloning efficiency. It will be of interest to determine if this functional change can be evoked or combined with more targeted approaches of epigenetic erasure.

ACKNOWLEDGMENT

We are grateful to our laboratory (J. Oliver) and farm (M. Berg, K. Cockrem, J. Forsyth) staff for excellent technical assistance. We thank Drs. H. Henderson, N. Cox, and P. Maclean for help with statistical analysis. Drs. D. Tremethick and T. Jenuwein kindly donated anti-H2A.Z and various anti-histone methylation antibodies, respectively.

REFERENCES

1. Bernstein BE, Meissner A, Lander ES. The mammalian epigenome. Cell 2007; 128:669–681.
2. Dinnyes A, Tian XC, Oback B. Nuclear Transfer for Cloning Animals. In: Meyers R (ed.), Reviews in Cell Biology and Molecular Medicine. Hoboken, NJ: John Wiley and Sons; 2016:2:76–117.
3. Chan MM, Smith ZD, Egli D, Regev A, Meissner A. Mouse ooplasm confers context-specific reprogramming capacity. Nat Genet 2012; 44: 978–980.
4. Kang YK, Lee KK, Han YM. Reprogramming DNA methylation in the preimplantation stage: peeping with Dolly's eyes. Curr Opin Cell Biol 2003; 15:290–295.
5. Santos F, Zakhartchenko V, Stojkovic M, Peters A, Jenuwein T, Wolf E, Reik W, Dean W. Epigenetic marking correlates with developmental potential in cloned bovine preimplantation embryos. Curr Biol 2003; 13: 1116–1121.
6. Fukuda A, Cao F, Morita S, Yamada K, Jincho Y, Tane S, Sotomaru Y, Kono T. Identification of inappropriately reprogrammed genes by large-scale transcriptome analysis of individual cloned mouse blastocysts. PLoS ONE 2010; 5:e11274.
7. Oback B. Climbing mount efficiency–small steps, not giant leaps towards higher cloning success in farm animals. Reprod Domest Anim 2008; 43(Suppl 2):407–416.
8. Tobey RA, Anderson EC, Petersen DF. Properties of mitotic cells prepared by mechanically shaking monolayer cultures of Chinese hamster cells. J Cell Physiol 1967; 70:63–68.
9. Lala PK. Studies on tumor cell population kinetics. In: Busch H (ed.), Methods in Cancer Research, vol. 6. New York: Academic Press; 1971:3–95.
10. Coller HA, Sang L, Roberts JM. A new description of cellular quiescence. PLoS Biol 2006; 4:e83.
11. Liu H, Adler AS, Segal E, Chang HY. A transcriptional program mediating entry into cellular quiescence. PLoS Genet 2007; 3:e91.
12. Lemons JM, Feng XJ, Bennett BD, Legesse-Miller A, Johnson EL, Raitman I, Pollina EA, Rabitz HA, Rabinowitz JD, Coller HA. Quiescent fibroblasts exhibit high metabolic activity. PLoS Biol 2010; 8:e1000514.
13. Wilmut I, Schnieke AE, McWhir J, Kind AJ, Campbell KH. Viable offspring derived from fetal and adult mammalian cells. Nature 1997; 385: 810–813.
14. Baxter J, Sauer S, Peters A, John R, Williams R, Caparros ML, Arney K, Otte A, Jenuwein T, Merkenschlager M, Fisher AG. Histone hypomethylation is an indicator of epigenetic plasticity in quiescent lymphocytes. EMBO J 2004; 23:4462–4472.
15. Heyman Y, Zhou Q, Lebourhis D, Chavatte-Palmer P, Renard JP, Vignon X. Novel approaches and hurdles to somatic cloning in cattle. Cloning Stem Cells 2002; 4:47–55.
16. Tani T, Kato Y, Tsunoda Y. Direct exposure of chromosomes to nonactivated ovum cytoplasm is effective for bovine somatic cell nucleus reprogramming. Biol Reprod 2001; 64:324–330.
17. Kasinathan P, Knott JG, Wang Z, Jerry DJ, Robl JM. Production of calves from G1 fibroblasts. Nat Biotechnol 2001; 19:1176–1178.
18. Cibelli JB, Stice SL, Golueke PJ, Kane JJ, Jerry J, Blackwell C, Ponce de Leon FA, Robl JM. Cloned transgenic calves produced from nonquiescent fetal fibroblasts. Science 1998; 280:1256–1258.
19. Wakayama T, Rodriguez I, Perry AC, Yanagimachi R, Mombaerts P. Mice cloned from embryonic stem cells. Proc Natl Acad Sci U S A 1999; 96:14984–14989.
20. Simon JA, Kingston RE. Mechanisms of polycomb gene silencing: knowns and unknowns. Nat Rev Mol Cell Biol 2009; 10:697–708.
21. Kuzmichev A, Margueron R, Vaquero A, Preissner TS, Scher M, Kirmizis A, Ouyang X, Brockdorff N, Abate-Shen C, Farnham P, Reinberg D. Composition and histone substrates of polycomb repressive group complexes change during cellular differentiation. Proc Natl Acad Sci U S A 2005; 102:1859–1864.
22. Margueron R, Reinberg D. The Polycomb complex PRC2 and its mark in life. Nature 2011; 469:343–349.
23. Bannister AJ, Kouzarides T. Regulation of chromatin by histone modifications. Cell Res 2011; 21:381–395.

24. Shahbazian MD, Grunstein M. Functions of site-specific histone acetylation and deacetylation. Annu Rev Biochem 2007; 76:75–100.
25. Sims RJ III, Reinberg D. Is there a code embedded in proteins that is based on post-translational modifications? Nat Rev Mol Cell Biol 2008; 9: 815–820.
26. Lee JS, Smith E, Shilatifard A. The language of histone crosstalk. Cell 2010; 142:682–685.
27. Wells DN, Laible G, Tucker FC, Miller AL, Oliver JE, Xiang T, Forsyth JT, Berg MC, Cockrem K, L'Huillier PJ, Tervit HR, Oback B. Coordination between donor cell type and cell cycle stage improves nuclear cloning efficiency in cattle. Theriogenology 2003; 59:45–59.
28. Jeon HY, Hyun SH, Lee GS, Kim HS, Kim S, Jeong YW, Kang SK, Lee BC, Han JY, Ahn C, Hwang WS. The analysis of telomere length and telomerase activity in cloned pigs and cows. Mol Reprod Dev 2005; 71: 315–320.
29. Oback B, Wells DN. Cloning cattle. Cloning Stem Cells 2003; 5:243–256.
30. Schurmann A, Wells DN, Oback B. Early zygotes are suitable recipients for bovine somatic nuclear transfer and result in cloned offspring. Reproduction 2006; 132:839–848.
31. Thompson JG, McNaughton C, Gasparrini B, McGowan LT, Tervit HR. Effect of inhibitors and uncouplers of oxidative phosphorylation during compaction and blastulation of bovine embryos cultured in vitro. J Reprod Fertil 2000; 118:47–55.
32. Robertson I, Nelson R. Certification and identification of embryos. In: Stringfellow DA, Givens MD (eds.), Manual of the International Embryo Transfer Society: A Procedural Guide and General Information for the Use of Embryo Transfer Technology, Emphasizing Sanitary Precautions, 4th ed. Champaign, IL: International Embryo Transfer Society; 2011:86–105.
33. Misica-Turner PM, Oback FC, Eichenlaub M, Wells DN, Oback B. Aggregating embryonic but not somatic nuclear transfer embryos increases cloning efficiency in cattle. Biol Reprod 2007; 76:268–278.
34. Eskeland R, Leeb M, Grimes GR, Kress C, Boyle S, Sproul D, Gilbert N, Fan Y, Skoultchi AI, Wutz A, Bickmore WA. Ring1B compacts chromatin structure and represses gene expression independent of histone ubiquitination. Mol Cell 2010; 38:452–464.
35. Suto RK, Clarkson MJ, Tremethick DJ, Luger K. Crystal structure of a nucleosome core particle containing the variant histone H2A.Z. Nat Struct Biol 2000; 7:1121–1124.
36. Shen X, Liu Y, Hsu YJ, Fujiwara Y, Kim J, Mao X, Yuan GC, Orkin SH. EZH1 mediates methylation on histone H3 lysine 27 and complements EZH2 in maintaining stem cell identity and executing pluripotency. Mol Cell 2008; 32:491–502.
37. Ma P, Schultz RM. Histone deacetylase 1 (HDAC1) regulates histone acetylation, development, and gene expression in preimplantation mouse embryos. Dev Biol 2008; 319:110–120.
38. Rothbart SB, Krajewski K, Nady N, Tempel W, Xue S, Badeaux AI, Barsyte-Lovejoy D, Martinez JY, Bedford MT, Fuchs SM, Arrowsmith CH, Strahl BD. Association of UHRF1 with methylated H3K9 directs the maintenance of DNA methylation. Nat Struct Mol Biol 2012; 19: 1155–1160.
39. Lehnertz B, Ueda Y, Derijck AA, Braunschweig U, Perez-Burgos L, Kubicek S, Chen T, Li E, Jenuwein T, Peters AH. Suv39h-mediated histone H3 lysine 9 methylation directs DNA methylation to major satellite repeats at pericentric heterochromatin. Curr Biol 2003; 13:1192–1200.
40. Hathaway NA, Bell O, Hodges C, Miller EL, Neel DS, Crabtree GR. Dynamics and memory of heterochromatin in living cells. Cell 2012; 149: 1447–1460.
41. McLean Z, Meng F, Henderson H, Turner P, Oback B. Increased MAP kinase inhibition enhances epiblast-specific gene expression in bovine blastocysts. Biol Reprod 2014; 91:49.
42. Smith C, Berg D, Beaumont S, Standley NT, Wells DN, Pfeffer PL. Simultaneous gene quantitation of multiple genes in individual bovine nuclear transfer blastocysts. Reproduction 2007; 133:231–242.
43. Saitou M, Barton SC, Surani MA. A molecular programme for the specification of germ cell fate in mice. Nature 2002; 418:293–300.
44. Hanna JH, Saha K, Jaenisch R. Pluripotency and cellular reprogramming: facts, hypotheses, unresolved issues. Cell 2010; 143:508–525.
45. Couldrey C, Lee RS. DNA methylation patterns in tissues from mid-gestation bovine foetuses produced by somatic cell nuclear transfer show subtle abnormalities in nuclear reprogramming. BMC Dev Biol 2010; 10: 27.
46. Antony J, Oback F, Chamley LW, Oback B, Laible G. Transient JMJD2B-mediated reduction of H3K9me3 levels improves reprogramming of embryonic stem cells into cloned embryos. Mol Cell Biol 2013; 33: 974–983.
47. Oback B, Wells DN. Donor cell differentiation, reprogramming, and cloning efficiency: elusive or illusive correlation? Mol Reprod Dev 2007; 74:646–654.
48. Collas P, Pinto-Correia C, Ponce de Leon FA, Robl JM. Effect of donor cell cycle stage on chromatin and spindle morphology in nuclear transplant rabbit embryos. Biol Reprod 1992; 46:501–511.
49. Boquest AC, Day BN, Prather RS. Flow cytometric cell cycle analysis of cultured porcine fetal fibroblast cells. Biol Reprod 1999; 60:1013–1019.
50. Katska L, Bochenek M, Kania G, Rynska B, Smorag Z. Flow cytometric cell cycle analysis of somatic cells primary cultures established for bovine cloning. Theriogenology 2002; 58:1733–1744.
51. Rubin H, Steiner R. Reversible alterations in the mitotic cycle of chick embryo cells in various states of growth regulation. J Cell Physiol 1975; 85:261–270.
52. Kubota C, Yamakuchi H, Todoroki J, Mizoshita K, Tabara N, Barber M, Yang X. Six cloned calves produced from adult fibroblast cells after long-term culture. Proc Natl Acad Sci U S A 2000; 97:990–995.
53. Raza A, Ucar K, Bhayana R, Kempski M, Preisler HD. Utility and sensitivity of anti BrdU antibodies in assessing S-phase cells compared to autoradiography. Cell Biochem Funct 1985; 3:149–153.
54. Zhu B, Reinberg D. Epigenetic inheritance: uncontested? Cell Res 2011; 21:435–441.
55. Jasencakova Z, Groth A. Restoring chromatin after replication: how new and old histone marks come together. Semin Cell Dev Biol 2010; 21: 231–237.
56. Maeshima K, Iino H, Hihara S, Funakoshi T, Watanabe A, Nishimura M, Nakatomi R, Yahata K, Imamoto F, Hashikawa T, Yokota H, Imamoto N. Nuclear pore formation but not nuclear growth is governed by cyclin-dependent kinases (Cdks) during interphase. Nat Struct Mol Biol 2010; 17: 1065–1071.
57. Wu RS, Tsai S, Bonner WM. Patterns of histone variant synthesis can distinguish G0 from G1 cells. Cell 1982; 31:367–374.
58. Ogawa H, Ishiguro K, Gaubatz S, Livingston DM, Nakatani Y. A complex with chromatin modifiers that occupies E2F- and Myc-responsive genes in G0 cells. Science 2002; 296:1132–1136.
59. Takahashi Y, Rayman JB, Dynlacht BD. Analysis of promoter binding by the E2F and pRB families in vivo: distinct E2F proteins mediate activation and repression. Genes Dev 2000; 14:804–816.
60. Cao R, Wang L, Wang H, Xia L, Erdjument-Bromage H, Tempst P, Jones RS, Zhang Y. Role of histone H3 lysine 27 methylation in Polycomb-group silencing. Science 2002; 298:1039–1043.
61. Stock JK, Giadrossi S, Casanova M, Brookes E, Vidal M, Koseki H, Brockdorff N, Fisher AG, Pombo A. Ring1-mediated ubiquitination of H2A restrains poised RNA polymerase II at bivalent genes in mouse ES cells. Nat Cell Biol 2007; 9:1428–1435.
62. Creyghton MP, Markoulaki S, Levine SS, Hanna J, Lodato MA, Sha K, Young RA, Jaenisch R, Boyer LA. H2AZ is enriched at polycomb complex target genes in ES cells and is necessary for lineage commitment. Cell 2008; 135:649–661.
63. Ogura A, Inoue K, Wakayama T. Recent advancements in cloning by somatic cell nuclear transfer. Philos Trans R Soc Lond B Biol Sci 2013; 368:20110329.
64. Bui HT, Wakayama S, Kishigami S, Park KK, Kim JH, Thuan NV, Wakayama T. Effect of trichostatin A on chromatin remodeling, histone modifications, DNA replication, and transcriptional activity in cloned mouse embryos. Biol Reprod 2010; 83:454–463.
65. Zhao J, Ross JW, Hao Y, Spate LD, Walters EM, Samuel MS, Rieke A, Murphy CN, Prather RS. Significant improvement in cloning efficiency of an inbred miniature pig by histone deacetylase inhibitor treatment after somatic cell nuclear transfer. Biol Reprod 2009; 81:525–530.
66. Costa Y, Ding J, Theunissen TW, Faiola F, Hore TA, Shliaha PV, Fidalgo M, Saunders A, Lawrence M, Dietmann S, Das S, Levasseur DN, et al. NANOG-dependent function of TET1 and TET2 in establishment of pluripotency. Nature 2013; 495:370–374.
67. Ficz G, Hore TA, Santos F, Lee HJ, Dean W, Arand J, Krueger F, Oxley D, Paul YL, Walter J, Cook SJ, Andrews S, et al. FGF signaling inhibition in ESCs drives rapid genome-wide demethylation to the epigenetic ground state of pluripotency. Cell Stem Cell 2013; 13:351–359.
68. Leitch HG, McEwen KR, Turp A, Encheva V, Carroll T, Grabole N, Mansfield W, Nashun B, Knezovich JG, Smith A, Surani MA, Hajkova P. Naive pluripotency is associated with global DNA hypomethylation. Nat Struct Mol Biol 2013; 20:311–316.
69. Chen J, Liu H, Liu J, Qi J, Wei B, Yang J, Liang H, Chen Y, Wu Y, Guo L, Zhu J, Zhao X, et al. H3K9 methylation is a barrier during somatic cell reprogramming into iPSCs. Nat Genet 2013; 45:34–42.
70. Soufi A, Donahue G, Zaret KS. Facilitators and impediments of the pluripotency reprogramming factors' initial engagement with the genome. Cell 2012; 151:994–1004.

71. Sridharan R, Gonzales-Cope M, Chronis C, Bonora G, McKee R, Huang C, Patel S, Lopez D, Mishra N, Pellegrini M, Carey M, Garcia BA, et al. Proteomic and genomic approaches reveal critical functions of H3K9 methylation and heterochromatin protein-1gamma in reprogramming to pluripotency. Nat Cell Biol 2013; 15:872–882.
72. Blelloch R, Wang Z, Meissner A, Pollard S, Smith A, Jaenisch R. Reprogramming efficiency following somatic cell nuclear transfer is influenced by the differentiation and methylation state of the donor nucleus. Stem Cells 2006; 24:2007–2013.
73. Matoba S, Liu Y, Lu F, Iwabuchi KA, Shen L, Inoue A, Zhang Y. Embryonic development following somatic cell nuclear transfer impeded by persisting histone methylation. Cell 2014; 159:884–895.
74. Tang F, Barbacioru C, Bao S, Lee C, Nordman E, Wang X, Lao K, Surani MA. Tracing the derivation of embryonic stem cells from the inner cell mass by single-cell RNA-Seq analysis. Cell Stem Cell 2010; 6:468–478.
75. Smith ZD, Chan MM, Mikkelsen TS, Gu H, Gnirke A, Regev A, Meissner A. A unique regulatory phase of DNA methylation in the early mammalian embryo. Nature 2012; 484:339–344.
76. Wang T, Chen K, Zeng X, Yang J, Wu Y, Shi X, Qin B, Zeng L, Esteban MA, Pan G, Pei D. The histone demethylases Jhdm1a/1b enhance somatic cell reprogramming in a vitamin-C-dependent manner. Cell Stem Cell 2011; 9:575–587.
77. Liang G, He J, Zhang Y. Kdm2b promotes induced pluripotent stem cell generation by facilitating gene activation early in reprogramming. Nat Cell Biol 2012; 14:457–466.
78. Sridharan R, Gonzales-Cope M, Chronis C, Bonora G, McKee R, Huang C, Patel S, Lopez D, Mishra N, Pellegrini M, Carey M, Garcia BA, et al. Proteomic and genomic approaches reveal critical functions of H3K9 methylation and heterochromatin protein-1gamma in reprogramming to pluripotency. Nat Cell Biol 2013; 15:872–882.
79. Epsztejn-Litman S, Feldman N, Abu-Remaileh M, Shufaro Y, Gerson A, Ueda J, Deplus R, Fuks F, Shinkai Y, Cedar H, Bergman Y. De novo DNA methylation promoted by G9a prevents reprogramming of embryonically silenced genes. Nat Struct Mol Biol 2008; 15:1176–1183.
80. Ma DK, Chiang C-HJ, Ponnusamy K, Ming GL, Song H. G9a and Jhdm2a regulate embryonic stem cell fusion-induced reprogramming of adult neural stem cells. Stem Cells 2008; 26:2131–2141.
81. Scharf AN, Barth TK, Imhof A. Establishment of histone modifications after chromatin assembly. Nucleic Acids Res 2009; 37:5032–5040.
82. Gaynor P, Wells DN, Oback B. Couplet alignment and improved electrofusion by dielectrophoresis for a zona-free high-throughput cloned embryo production system. Med Biol Eng Comput 2005; 43:150–154.
83. Ogura A, Inoue K, Ogonuki N, Lee J, Kohda T, Ishino F. Phenotypic effects of somatic cell cloning in the mouse. Cloning Stem Cells 2002; 4: 397–405.
84. Wells DN, Forsyth JT, McMillan V, Oback B. The health of somatic cell cloned cattle and their offspring. Cloning Stem Cells 2004; 6:101–110.
85. Gibbons J, Arat S, Rzucidlo J, Miyoshi K, Waltenburg R, Respess D, Venable A, Stice S. Enhanced survivability of cloned calves derived from roscovitine-treated adult somatic cells. Biol Reprod 2002; 66:895–900.
86. Cooper S. Mammalian cells are not synchronized in G1-phase by starvation or inhibition: considerations of the fundamental concept of G1-phase synchronization. Cell Prolif 1998; 31:9–16.